Cell-cycle-dependent dynamics of nuclear pores: pore-free islands and lamins

Kazuhiro Maeshima[1,*], Kazuhide Yahata[2], Yoko Sasaki[1], Reiko Nakatomi[3], Taro Tachibana[4], Tsutomu Hashikawa[3], Fumio Imamoto[2] and Naoko Imamoto[1,*]

[1]Cellular Dynamics Laboratory, Discovery Research Institute, RIKEN, 2-1 Hirosawa, Wako-shi, Saitama, 351-0198 Japan
[2]Department of Molecular Biology, BIKEN, Osaka University, Osaka, Japan
[3]Laboratory for Neural Architecture, Brain Research Institute, RIKEN, Wako-shi, Japan
[4]Department of Bioengineering, Graduate School of Engineering, Osaka City University, Osaka, Japan
*Authors for correspondence (e-mail: maeshima@riken.jp; nimamoto@riken.jp)

Accepted 9 August 2006
Journal of Cell Science 119, 4442-4451 Published by The Company of Biologists 2006
doi:10.1242/jcs.03207

Summary

Nuclear pores are sophisticated gateways on the nuclear envelope that control macromolecular transport between the cytoplasm and nucleoplasm. So far the structural and functional aspects of nuclear pores have been extensively studied, but their distribution and density, which might reflect nuclear organization and function, remain unknown. Here, we report the cell-cycle-dependent dynamics of nuclear pores. Large distinct subdomains lacking nuclear pores are present on the nuclear surface of HeLaS3 cells in early cell-cycle stages. Such 'pore-free islands' gradually become dispersed in G1-S phase. Surprisingly, the islands are enriched with inner nuclear membrane proteins lamin A/C and emerin, but exclude lamin B. Lamin-A/C-enriched pore-free islands were also observed in human normal diploid fibroblasts and several cell lines, showing the generality of this phenomenon. Knockdown and ectopic expression analyses demonstrated that lamin A/C, but not emerin, plays an essential structural and regulatory role in the nuclear pore distribution and the formation of pore-free islands. These data thus provide strong evidence that the dynamics of nuclear pores are regulated by the reorganization of inner nuclear structures.

Supplementary material available online at
http://jcs.biologists.org/cgi/content/full/119/21/4442/DC1

Key words: Emerin, Cell cycle, Lamin A/C and lamin B, Nuclear pores, Nuclear structure

Introduction

The eukaryotic nucleus is a complex and sophisticated organelle that contains genomic chromatin, and supports many essential cellular activities, including DNA replication, RNA transcription and processing, and ribosome assembly. Such nuclear functions are largely dependent upon the structural organization of the nucleus and the formation of a membranous structure, the nuclear envelope (NE), which separates the nucleoplasm from the cytoplasm (Gerace and Burke, 1988). The nuclear envelope consists of an inner and outer nuclear membrane, nuclear pores, and the underlying nuclear lamina, a filamentous meshwork (Goldman et al., 2002).

The core meshwork structure of the lamina is formed by type-V intermediate filament proteins called lamins, which are composed of B-type (lamin B1-3) and A-type lamins (lamin A and its short splicing variant, lamin C) (Aebi et al., 1986; Stuurman et al., 1998). While B-type lamins are constitutively expressed in cells throughout development, A-type lamins (lamin A/C) are only expressed in later stages of development and in differentiated cells (Hutchison et al., 2001). The importance of lamins has been demonstrated by several recent findings: genetic approaches in *Drosophila melanogaster* (Lenz-Bohme et al., 1997), *Caenorhabditis elegans* (Liu et al., 2000), and cultured mammalian cells (Harborth et al., 2001), all of which suggest that B-type lamins are essential for viability. The targeted disruption of lamin A/C in mice causes muscular dystrophy, loss of adipose tissue and early death (Sullivan et al., 1999). In addition, mutations in the lamin A/C gene, as well as in several genes that encode inner nuclear membrane proteins that bind to the lamina, have been shown to cause a variety of human genetic disorders: the so-called 'laminopathies', including Emery-Dreifuss muscular dystrophy and Hutchinson-Gilford progeria syndrome (HGPS) (Burke and Stewart, 2002; Hutchison and Worman, 2004; Mounkes et al., 2003; Wilson, 2000).

In addition to the nuclear membrane and the nuclear lamina, nuclear pores are genuine constituents of the nuclear envelope. In eukaryotic cells, all macromolecules that are transported between the nucleus and the cytoplasm cross the nuclear membrane through nuclear pore complexes (NPCs) (Imamoto, 2000). NPCs are elaborate gateways that allow the translocation of a variety of macromolecules in an efficient but selective fashion (Cronshaw et al., 2002; Gorlich and Kutay, 1999; Macara, 2001; Rout et al., 2000). In vertebrate cells, NPCs are cylindrical structures consisting of multiple copies of about 30 different proteins called nucleoporins, with a diameter of 120 nm, a thickness of 70 nm, and a mass of approximately 100 MDa (Davis, 1995; Fahrenkrog et al., 2004; Hetzer et al., 2005; Rout and Wente, 1994; Suntharalingam and Wente, 2003; Vasu and Forbes, 2001). However, how, when and where these nucleoporins converge

to form a nuclear pore remains largely unknown. Once formed on the nuclear membrane, NPCs have static and immobile nature, suggesting that they are physically linked to intranuclear structures such as the nuclear lamina, inner nuclear membrane proteins, and chromatins (Daigle et al., 2001; Rabut et al., 2004).

Since a number of previous studies have just focused on gating properties and structural analyses of nuclear pores to understand the transport mechanism, exploring the behavior of nuclear pores would also be of interest. Several earlier reports demonstrated that the number of nuclear pores increases during the cell cycle (Maul et al., 1971) or in response to hormone stimulation (Maul et al., 1980; Oberleithner et al., 1994). Highly proliferative cells such as embryos or tumors have a high density of nuclear pores, whereas terminal differentiated cells such as erythrocytes have much fewer (Maul et al., 1980). These observations imply that the density of nuclear pores might be correlated with the cellular metabolic activity. More recently, it was shown that components of nuclear pores are implicated in the spatial gene regulation, suggesting the structural roles for nuclear pores in the nuclear organization and function (Casolari et al., 2004; Ishii et al., 2002; Schmid et al., 2006). These observations suggest a highly dynamic aspect of nuclear pores, and raise the question of whether certain cellular events can determine the behavior of nuclear pores.

To address this question, we investigated the dynamics of nuclear pore distribution and density in human cells. We initially found novel and unique subdomains on the nuclear envelope of HeLa S3 cells, which resembles large "islands" that are devoid of nuclear pores. An examination throughout the cell cycle revealed that such pore-free islands are present in the telophase and in most G1 phase nuclei. This pore-free island gradually disperses, and pore density concomitantly increases, as the cell cycle progresses to the S phase. Surprisingly, some inner nuclear membrane proteins including emerin and lamin A/C, but not lamin B, are highly enriched in the pore-free islands. Uneven distributions of nuclear pores and dynamic changes were also observed in human osteosarcoma U-2 OS and in human IMR90 normal diploid fibroblasts. siRNA-mediated knockdown of lamin A/C resulted in the disappearance of pore-free islands, whereas the upregulation of lamin A/C stabilized and/or facilitated formation of pore-free islands. Our present results show that lamin A/C plays an essential structural and regulatory role in pore distribution, and also determine the nuclear subdomains, where nucleocytoplasmic transport could be suppressed as a function of cell growth and differentiation.

Results

Dynamic change(s) of nuclear pore distributions during the cell cycle

With the recent development of fluorescence microscopy imaging, it has become possible to visualize a single nuclear pore on the nuclear surface, by immunostaining with antibodies that recognize the nuclear pore components (inset in Fig. 1A1) (Kubitscheck et al., 1996). To investigate nuclear pore distributions and density in a HeLa S3 cell line, nuclear pores in asynchronous cells were immunostained. Bright punctate rim

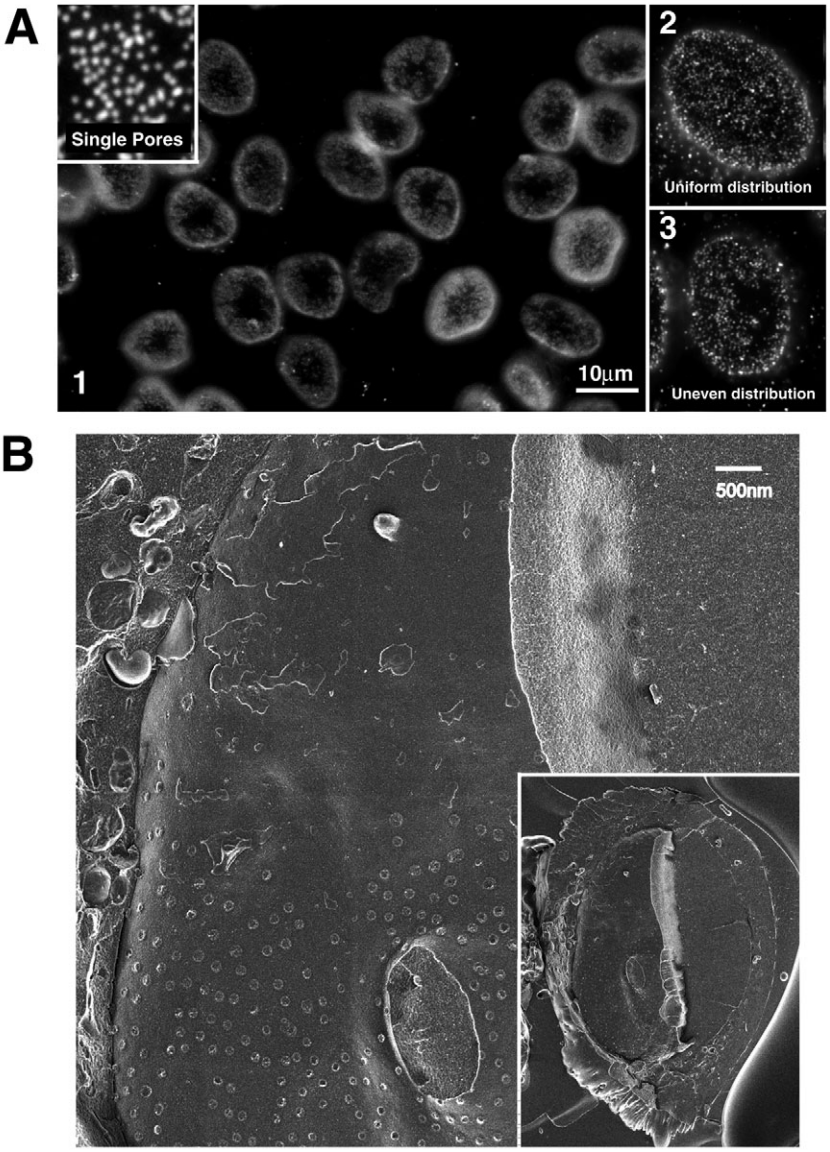

Fig. 1. Heterogeneous distribution of nuclear pores. (A1) Low-magnification image of asynchronous HeLa S3 nuclear surfaces stained for nuclear pores with anti-p62 antibody. Note that the nuclear pore distributions are surprisingly heterogeneous from nucleus to nucleus. Inset, visualization of single nuclear pores at high magnification. (A2) Nucleus with an almost uniform pore distribution. (A3) Nucleus with a large 'island' that is devoid of nuclear pores. (B) Direct observation of nuclear pores and pore-free islands by scanning electron microscopy. A nuclear surface of freeze-fractured early G1 HeLaS3 cells (inset) and its enlarged image. Many nuclear pores are clearly visible. A large pore-free island is spread on the smooth inner nuclear envelope, demonstrating the integrity of the nuclear envelope.

staining was observed on the nuclear equator (supplementary material Fig. S1A). However, an examination of the nuclear surface (adjacent to the growth surface) revealed that the nuclear pores were strikingly unevenly distributed (Fig. 1A1): some nuclei showed an almost uniform pore distribution (Fig. 1A2), whereas other nuclei contain large 'islands' that are devoid of nuclear pores (Fig. 1A3). Such large pore-free islands comprise as much as 40% of the nuclear surface. These pore-free islands were also observed by a stable expression of nucleoporin p62 conjugated to Venus (a bright YFP derivative) (Nagai et al., 2002) in the HeLaS3 cells, ruling out the possibility that this is due to a staining artifact (supplementary material Fig. S1C). In addition to the visualization of nuclear pores by immunostaining and ectopic expression of fluorescent nucleoporin, freeze-fractured samples of HeLaS3 cells were prepared and observed by a cryo-scanning electron microscopy to directly visualize the nuclear pores and pore-free islands. An enlarged image (Fig. 1B) clearly demonstrates a large pore-free island spreading onto the smooth and continuous nuclear envelope.

If the nuclear pore distribution is assumed to be random and obey a Poisson distribution, the probability of forming a 30 μm^2 pore-free island, as is typically found, will be about 10^{-79} (see Materials and Methods). This implies that the pore-free island is not formed by chance. It is thus conceivable that a specific structure contributes to make the regions pore-free. What could cause such uneven pore distributions, forming pore-free islands? What is the structural organization of the pore-free islands? These questions were addressed in the following studies.

We first wondered whether differences in the pore distribution were correlated with cell cycle progression. To test this possibility, the distribution of nuclear pores throughout the HeLa S3 cell cycle was investigated using three cell cycle markers, Ki67, PCNA and CENP-F, which are useful in identifying the G1, S and G2 stages, respectively. The nuclei with small Ki-67 discrete foci characteristics of early G1 cells (Kill, 1996), have large pore-free islands on the nuclear surface (supplementary material Fig. S4A). A quantitative analysis showed that 90% of the early G1 nuclei contained such pore-free islands on the top and/or bottom surface (Table 1). In the early S-phase, PCNA foci are distributed throughout the nucleoplasm although they are absent in G1 and G2 nuclei. A nucleus with such PCNA foci has a smaller pore-free island whereas the paired nuclei without PCNA signal, presumably in the G1 phase, possess large pore-free islands on the surfaces (Fig. 2A). Nuclei in mid-to-late S phase, represented by PCNA foci that are larger in size and fewer in number (Dimitrova et al., 1999), show a much more uniform pore distribution and contain a number of small pore-free islands (Fig. 2A, top panels). The percentage of nuclei with large pore-free islands dropped to 26% at this stage (Table 1). G2-phase nuclei, which are highly positive for

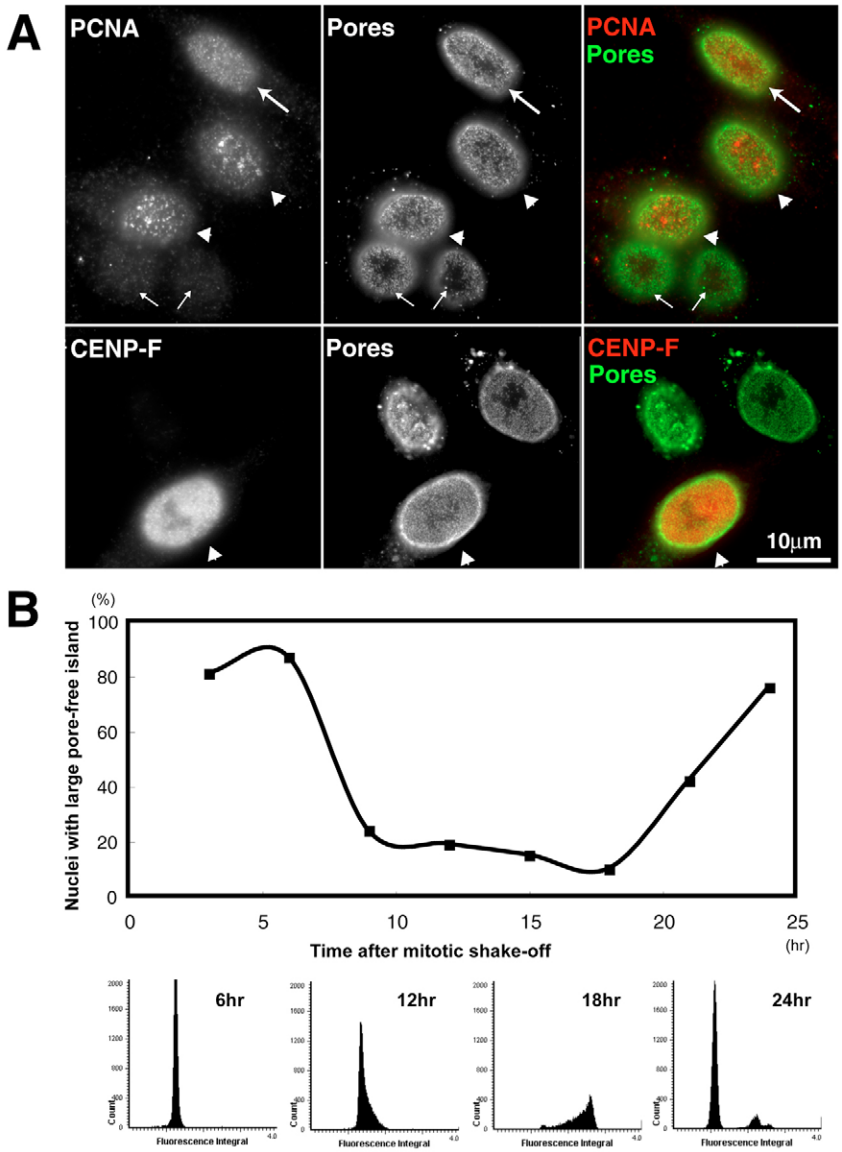

Fig. 2. (A) Cell-cycle dependency of nuclear pore distribution in HeLaS3 cells. Nuclei were co-stained for nuclear pores (center column) and PCNA (top panels) or G2 marker CENP-F (bottom panels). The paired nuclei without PCNA signal, probably in G1 phase, possess large pore-lacking islands (top panels, small arrows), whereas the nucleus with early-S PCNA foci (large arrows) has a smaller pore-free island. The two nuclei with large and few PCNA foci (top panels, arrowheads), characteristics of mid-late S-phase nuclei, have a much more uniform pore distribution. The nucleus with CENP-F signal has uniform pore distributions (bottom panels, arrowheads). Nuclei without CENP-F have large pore-free islands on the nuclear surface. Asynchronous cells were used in these experiments. (B) Dispersal of pore-free island with cell-cycle progression. Synchronized mitotic HeLaS3 cells were collected and released at 0 hour. After 3, 6, 9, 12, 15, 18, 21, 24 hours, the number of nuclei in which more than 30% of the surface is comprised of pore-free islands, was counted and shown as a percentage. Cell-cycle profiles of the released cells at the indicated time-points were obtained with an Olympus LCS2, demonstrating cell-cycle progress in a time-dependent manner (histograms).

Table 1. Quantitative analysis of the pore-free islands in various cell-cycle stages

Cell-cycle stage	Marker	Nuclei with pore-free islands*
Telophase and cytokinesis		100 / 100
Early G1	Ki-67	89 / 100
Early S	PCNA	50 / 100
Mid to late S	PCNA	26 / 100
G2	CENP-F	9 / 100
Late G2 to prophase†	CENP-F	6 / 100

*The number of nuclei in which more than 30% of the surface is comprised of pore-free islands (n=100 cells). †Nuclei with enrichments of CENP-F at the centromere regions.

CENP-F signals (Liao et al., 1995), show rather uniform pore distributions (Fig. 2A, bottom panels). At this stage, fewer than 10% of the nuclei contain pore-free islands on the surface (Table 1). The series of cell-cycle analysis evidently shows that pore-free islands disperse with cell-cycle progression. To confirm this finding, we collected synchronized mitotic cells, released them, and counted the number of nuclei with large pore-free island at various time points (Fig. 2B). In good agreement with the analysis using cell-cycle markers, the number of nuclei with large pore-free islands decreases with cell cycle progression.

A quantitative analysis revealed that the average pore density on the G1 nuclear surface, including the pore-free island, is about 5 NPCs/μm^2. The pore density in G2 cells increases to 8.56±0.34 NPCs/μm^2. The disappearance of the pore-free island is likely to be correlated with the increase in pore density (see below and Discussion). The nuclear pore distributions thus drastically change, from uneven to even, with increase in pore density as the cell cycle progresses in HeLa S3 cells.

Structural organization of the pore-free islands

As described above, HeLa S3 nuclei contain large pore-free islands in the early stages of the cell cycle. The next obvious question is what is the structural organization of the pore-free islands. To answer this question, the internal nuclear structure of the pore-free islands was examined by immunostaining several inner nuclear membrane proteins. Fig. 3A (fourth row) shows that lap2β is distributed almost uniformly on the nuclear surface in G1 phase, showing the integrity of the nuclear envelope. We found, however, that emerin and lamin A/C, which are linked to a variety of human genetic disorders (laminopathies) including Emery-Dreifuss muscular dystrophy, are highly enriched in the pore-free islands (Fig. 3A, first and third rows and supplementary material Fig. S1B). Co-immunostaining of nuclear pores and emerin or lamin A/C shows an apparently complementary pattern. Ectopic co-expression of CFP-emerin and p62-Venus also show a complementary pattern, confirming the immunostaining result (supplementary material Fig. S1C). At telophase, emerin accumulates in the pore-free islands on both sides of the newly reformed nuclei (Fig. 3A, second row). This observation is reminiscent of the 'core' region proposed by Haraguchi et al. (Haraguchi et al., 2000; Haraguchi et al., 2001), suggesting that the pore-free islands originate from the telophase

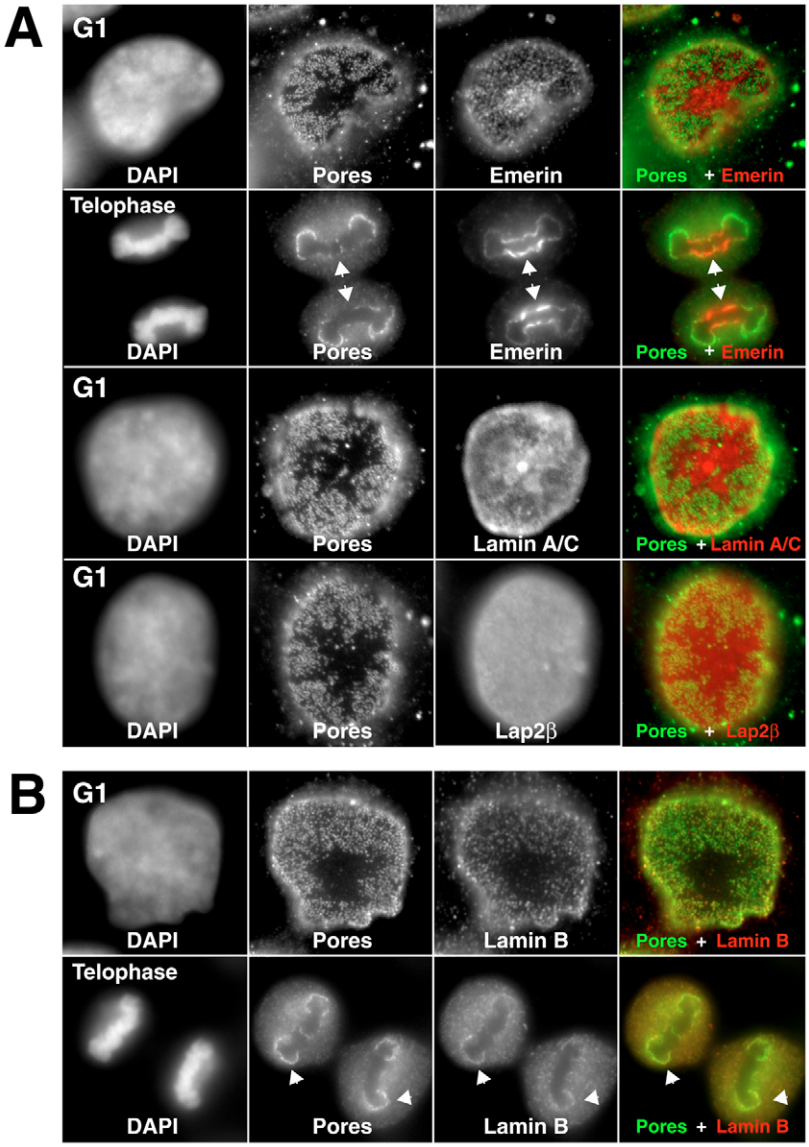

Fig. 3. Structural organization of pore-free islands. (A) Accumulation of inner nuclear membrane proteins emerin and lamin A/C in the pore-free islands. Nuclei co-stained for nuclear pores and inner nuclear membrane proteins: emerin (top two rows), lamin A/C (third row) and lap2β (fourth row). Emerin and lamin A/C are enriched in the pore-free islands of G1 (first and third rows) and telophase (second row) nuclei. Note that lap2β is almost uniformly distributed on the surface of the G1 nucleus (fourth row). (B) Lamin B is excluded from the pore-free island. Surface image of the G1 nuclei (top panels) and middle section of the telophase nuclei (bottom panels), co-stained with DAPI, nuclear pores and lamin B. Merged images of nuclear pores and lamin B are shown on the right. Note that nuclear pores colocalized well with lamin B both in telophase and G1 nuclei (arrowheads).

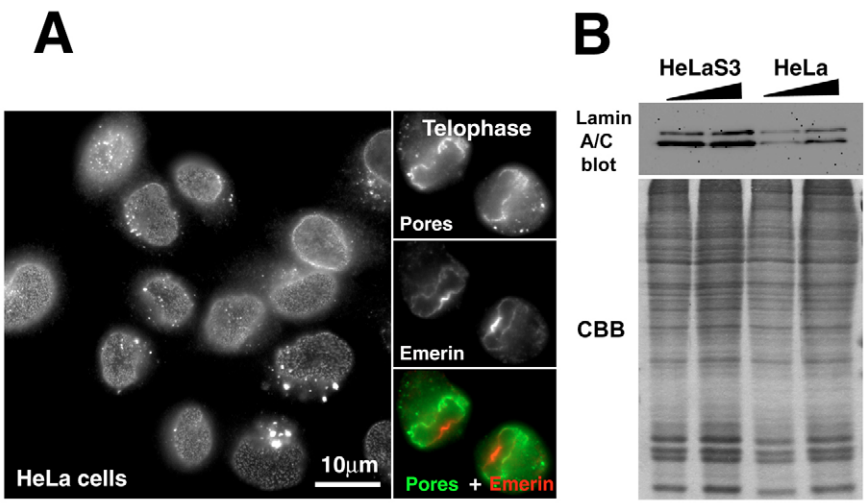

Fig. 4. Expression levels of lamin A/C affect the nuclear pore dynamics. (A) Low-magnification image of nuclear pore staining of asynchronous HeLa nuclear surfaces. The nuclear pores in most of the cells show more uniform distributions, compared with those of HeLa S3 cells shown in Fig. 1A and Fig. 3A. HeLa telophase nuclei co-stained for emerin and nuclear pores, demonstrated notable pore-free islands enriched with emerin ('core' regions) (right). (B) A-type lamins are upregulated by 4.25 times in HeLaS3 cells that contain distinct pore-free islands. Expression levels of lamin A/C in HeLaS3 cells (left two lanes) and the HeLa cells (right two lanes) shown in A were examined by western blotting. Cell lysate, equivalent to 0.5×10^4 (left) or 1×10^4 (right) cells, was loaded per lane for each cell type and verified by Coomassie Brilliant Blue (CBB) staining (bottom panel).

'core' regions. Notably, G1-phase nuclei possess emerin- and lamin A/C-accumulated islands on the top and bottom surfaces of the nuclei (Fig. 3A, first and third rows). This observation also suggests that telophase cells fall to one side and become flat during the progression from telophase to G1 phase. In contrast to A-type lamins, the staining signal for lamin B, which is an ubiquitously expressed lamin, was almost absent from the pore-free islands in both G1 and telophase nuclei, showing a very similar localization to that of the nuclear pores (Fig. 3B). Consistent with this result, lamin B receptor (LBR) is also localized in the pore region, which is complementary to the emerin staining (supplementary material Fig. S2A). We thus defined the pore-free islands as emerin- and lamin A/C-enriched areas.

Role of lamin A/C in the organization of the pore-free islands

In the course of our investigation, we noticed that some other HeLa cell lines show more-uniform pore distributions (Fig. 4A, left panel). In such HeLa cell lines, newly assembled nuclei in the telophase all contained large pore-free islands that were enriched with emerin (Fig. 4A, right panels). However, the timing of dispersal of the pore-free islands differed among HeLa cell lines and appeared to be correlated with their proliferation activity: cells that retain pore-free islands longer, have a lower proliferation activity, and vice versa (supplementary material Fig. S5C and also discussed below). In the most rapidly growing HeLa cells, the large pore-free islands appear to disperse rather quickly, consistent with the findings reported by Haraguchi et al. (Haraguchi et al., 2000; Haraguchi et al., 2001). Thus, some variations in the dynamics of nuclear pore distributions exist among HeLa cell lines. If so, what could cause such variation?

We were first concerned that the HeLa S3 cells underwent mutation(s) in the inner nuclear membrane proteins organizing the nuclear structure. To rule out this possibility, cDNAs of several inner nuclear membrane proteins (BAF, emerin, lamin A, lamin C) were isolated from the HeLa S3 cells and sequenced. No mutations were found in the sequences in any of these cDNAs (data not shown). The expression levels of the inner nuclear membrane proteins were next examined by western blotting. In the HeLa S3 cell line, the expression of lamin A/C is upregulated 4.25 times, compared with the HeLa cell line in which the pore-free islands disperse rather quickly (Fig. 4B).

To examine an involvement of lamin A/C in pore distribution more directly, we carried out the knockdown of emerin or lamin A/C using an siRNA system (Elbashir et al., 2001; Harborth et al., 2001). The reduction of emerin and lamin A/C were clearly observed within 72 hours of RNA transfection (Fig. 5A,B). In the emerin-reduced cells, the large pore-free islands were apparently unaffected (Fig. 5B). By contrast, in lamin-A/C-depleted cells (Fig. 5A), the pore-free islands were drastically dispersed. The enlarged images (Fig. 5A, bottom panels) show some narrow regions containing residual lamin A/C. The narrow regions are almost completely devoid of nuclear pores, showing they are organized in mutually exclusive patterns on the nuclear envelope. The cell-cycle profile of the lamin-A/C-knockdown cells was indistinguishable from that of control cells (Fig. 5A), excluding the possibility that S phase or G2 phase retardation in the knockdown cells could cause dispersion of the pore-free islands. These results demonstrate that lamin A/C has an essential role in the formation of pore-free islands and that emerin is just a 'passenger' on the islands without a direct activity in pore dynamics.

In a complementary experiment, we examined whether the ectopic expression of lamin A/C can induce pore-free islands in the HeLa cell line which possess uniformly distributed pores. For this, Venus-tagged lamin A driven by the EF1α promoter was transiently expressed in the HeLa cells and the nuclear pore distributions were then examined (Fig. 6). The expressed Venus-lamin A was located at the rim of the nuclei within 48 hours after transfection, indicating the successful incorporation of Venus-lamin-A into the nuclear envelope (not shown). On the surface of these nuclei, Venus-lamin-A were enriched in discrete regions, and nuclear pores were excluded from such lamin-A-enriched regions, leading to the formation of the pore-free islands (Fig. 6), whereas the localization of lamin B was rather similar to that of Venus-lamin-A (not shown). Moreover, the lamin-A enrichment induced the clustering of nuclear pores. These results demonstrate that an ectopic expression of lamin A effectively facilitates the formation of pore-free islands on the nuclear envelope. Considering the above findings, we conclude that lamin A/C

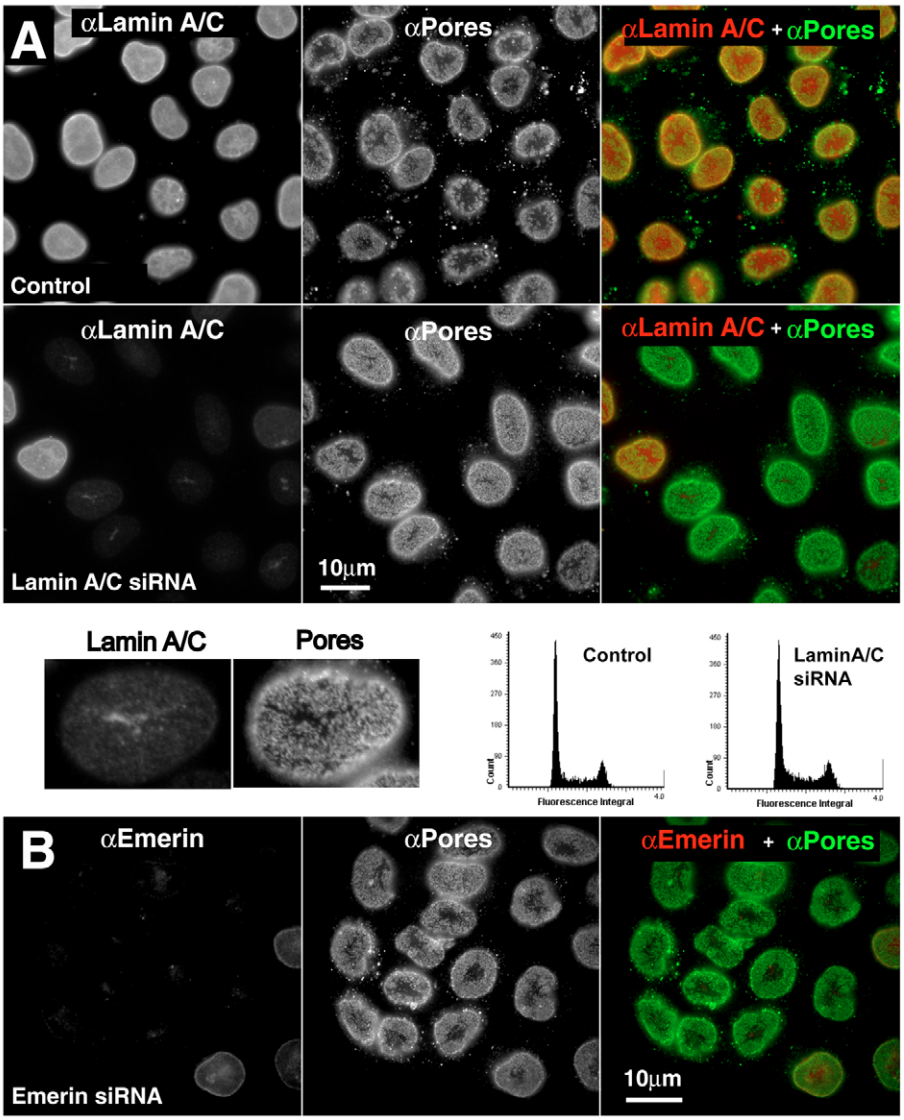

Fig. 5. Depletion of lamin A/C specifically disperses the pore-free island.
(A) Knockdown of lamin A/C by siRNA results in dispersal of the pore-free islands in HeLaS3 cells. Top panels, control cells (no RNA transfection) co-stained with nuclear pores (center) and lamin A/C (left). Bottom panels, siRNA-transfected cells co-stained with the same set of antibodies. Note that the pore-free islands in lamin A/C-depleted cells are significantly reduced. Lower images are enlarged images of a lamin A/C-reduced nucleus, showing a narrow region where residual lamin A/C has accumulated. This narrow region is almost completely devoid of nuclear pores. The histograms show DNA content of the control and knockdown cells, suggesting no significant difference in cell-cycle profile. (B) Knockdown of emerin in HeLaS3 cells. In contrast to the lamin A/C-depleted cells (A), the emerin-reduced cells still contain the large pore-free islands. This indicates that emerin itself is not directly involved in determining nuclear pore distribution.

could indeed control the nuclear pore distribution in HeLa cells.

Generality of nuclear pore dynamics and underlying structural organizations

It is of particular interest to know whether the uneven pore distributions and their cell-cycle-dependent dynamics are general phenomena. Examination of nuclear pore distributions in human osteosarcoma U-2 OS cells revealed conserved pore-free islands enriched with lamin A/C, and their dispersion induced by cell-cycle progression (supplementary material Fig. S2B). Similar observations were also obtained from a colorectal cancer cell-line HCT119 cells (not shown). In addition to these transformed cell lines, we examined IMR90, human normal diploid fibroblasts. In the early stage (telophase to G1), the nuclear pores show strikingly patched distributions (Fig. 7A and supplementary material Fig. S3). As is the case for HeLa cells, these uneven pore patterns apparently originate

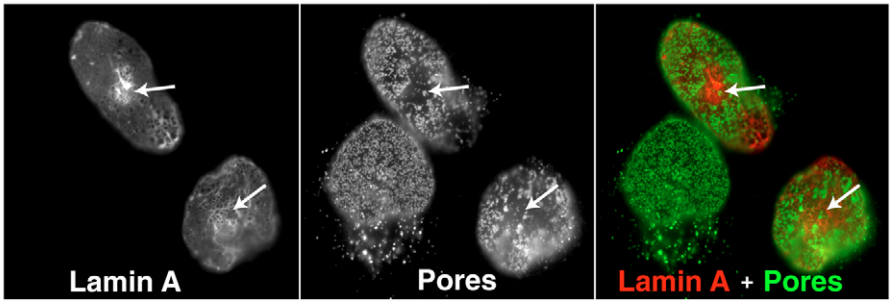

Fig. 6. Ectopic expression of lamin A induces formation of the pore-free islands. Transient expression of Venus-lamin-A in HeLa cells with uniform pore distributions. Nuclear surface images of HeLa cells (Fig. 4A) expressing Venus-lamin-A and stained for nuclear pores. Enrichment of expressed Venus-lamin-A induces distinct pore-free islands (arrows).

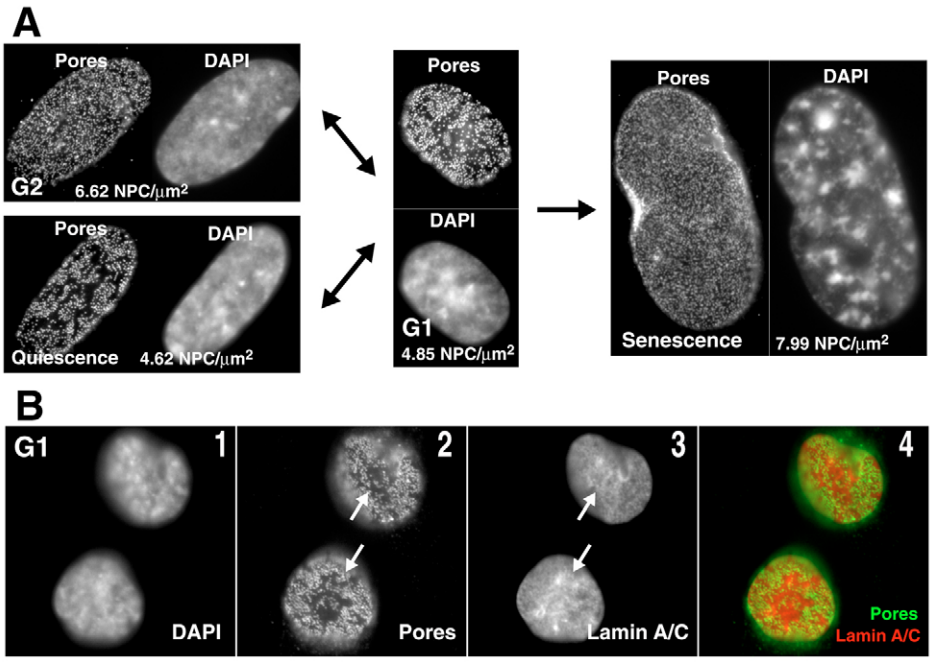

Fig. 7. Conserved structure and dynamics of pore-free islands in human normal diploid fibroblast IMR90 cells. (A) Dynamic changes in nuclear pore distributions during the cell cycle of human normal diploid IMR90 fibroblasts. In the G1 nucleus (center), the pore distribution displayed a patched pattern (see also supplementary material Fig. S3), but upon cell-cycle progression, pore distribution becomes uniform, coupled with an increase in pore number (top left). Quiescent cells induced by serum depletion still have patched pore distribution (bottom left), whereas the senescent cell nucleus shows a uniform pore distribution with a high density of pores (right). Note that DAPI staining of the senescent nucleus shows typical heterochromatic foci in the nucleoplasm (SAHF). (B) Lamin A/C is enriched in the pore-free islands of G1 nuclei of IMR90 cells (arrows), suggesting the structural conservation of the pore-free islands. 1, DAPI; 2, nuclear pores; 3, lamin A/C; 4, merged images of nuclear pores and lamin A/C.

from the beginning of telophase, when nuclear pores and lamin A/C are recruited to the surface of chromosome clusters (or mass) in a mutually exclusive manner (supplementary material Fig. S3). The pore density in early G1 is 4.85±0.40 NPCs/μm^2 (Fig. 7A). The pore distributions then become uniform in a later stage (G2), with an increase in pore density to 6.62±0.47 NPCs/μm^2, showing that such nuclear pore dynamics are ubiquitous in human cell lines.

Interestingly, in the replicative senescent state, the distribution of nuclear pores becomes much more uniform, with increased pore density to 7.99±0.18 NPCs/μm^2, whereas the distribution and density of pores in the quiescent cells (G0) by serum depletion remained very similar to those of G1 nuclei (4.62±0.44 NPCs/μm^2). The patched pattern of the uneven pore distribution is thus more prominent in the early stage of the cell cycle, and is maintained in the quiescent state (G0). Notably the patched pore pattern in the quiescent cells is easily reversed to the normal cell cycle state by serum add-back. With the progression of the cell cycle, or in the replicative senescent state, the patched pattern became dispersed, probably coupled with an increase in pore number. These findings indicate that the distribution and density of nuclear pores in the normal diploid cells significantly change during the cell-cycle progression and upon the physiological state of the cells. Moreover, lamin A/C accumulates in the pore-free islands, in the early stages of IMR90 (Fig. 7B). These results clearly show the generality of structural organization and dynamics of pore-free islands.

Discussion

Emerin, lamin A/C, and lamin B in the pore-free islands

In this study, we investigated cell-cycle-dependent dynamics of nuclear pores and found novel subdomain (island) of the nuclear envelope in human normal diploid fibroblasts IMR90 and other cell lines. The islands are devoid of nuclear pores and enriched with inner nuclear membrane proteins emerin and lamin A/C (Figs 2-3 and supplementary material Fig. S1B,C). The siRNA-mediated knockdown of lamin A/C in the cells led to dispersal of the pore-free islands (Fig. 5A). It should be noted that the knockdown of lamin A/C did not affect the cell growth (Harborth et al., 2001) (not shown) and cell-cycle profile (Fig. 5A). By contrast, a reduction in emerin did not have a significant effect on the islands (Fig. 5B). This is not so surprising for the following reasons. Consistent with previous reports (Harborth et al., 2001; Sullivan et al., 1999), the knockdown of lamin A/C strongly enhanced an unusual cytoplasmic distribution of emerin (not shown). However, a reduction in emerin levels had no influence on the localization of lamin A/C, indicating that lamin A/C serves to immobilize emerin. Moreover, an ectopic expression of lamin A had a significant effect on the distribution of nuclear pores (Fig. 6). Lamin A/C thus plays a dominant role in the formation of the pore-free islands, possibly in cooperation with other inner nuclear membrane proteins such as lamin binding proteins (LAPs).

Interestingly, the staining of lamin B, which is a constitutively expressed B-type lamin (Harborth et al., 2001; Lenz-Bohme et al., 1997; Liu et al., 2000) and lamin B receptor (LBR), indicate that it is rarely located in the pore-free islands in HeLa S3 cells (Fig. 3B and supplementary material Fig. S2A). This suggests that A-type and B-type lamins are preferentially incorporated into rather discrete regions on the inner nuclear envelope, having a surprisingly clear correlation with the nuclear pore distribution. Several studies have reported that lamin B could be associated with the nuclear pores, through some nucleoporins (Hawryluk-Gara et al., 2005; Smythe et al., 2000). Their interaction(s) might imply a role for lamin B in recruiting and/or the spacing of nuclear pores, as obtained from genetic evidence (Lenz-Bohme et al., 1997; Liu et al., 2000). Our results also suggest a clear functional

difference, regarding pore formation, between lamin B and lamin A/C that is generally expressed in differentiated cells.

Regulation of nuclear pore distributions and density by lamin A/C

As shown in supplementary material Fig. S5C, we observed that HeLa cells with lower amounts of lamin A/C and uniform pore distribution, have a higher proliferation activity than HeLa S3 and U2-OS cells. In good agreement with our observations, embryonic cells whose nuclei lack A-type lamins have a much higher nuclear pore density (40-50 NPCs/μm^2) and proliferation activity (Maul et al., 1980). Furthermore, several studies have reported that the absence or downregulation of lamin A/C is correlated with rapid growth or aggressivity in human malignancies including small-cell lung carcinoma (Broers and Ramaekers, 1994), testicular cancer (Machiels et al., 1997), leukemias and lymphomas (Stadelmann et al., 1990) and skin carcinomas (Venables et al., 2001). These reports support the hypothesis that lamin A/C has a negative influence on cell proliferation. The suppression of lamin A/C might contribute to tumorigenesis through increasing pore density. It was recently reported that the epigenetic silencing of the lamin A/C gene by CpG island promoter hypermethylation is responsible for the loss of expression in leukemias and lymphomas (Agrelo et al., 2005). Such epigenetic effects might cause variations of lamin A/C expression in HeLa cells.

Dynamic change(s) of the pore-free islands during the cell cycle

In the present study, we show that lamin A/C plays an essential structural and regulatory role in the formation of the pore-free islands. Besides lamin A/C, what else would be involved in the event? Interestingly, many Ki-67 punctuate foci are also localized in the pore-free islands in the early G1 phase (supplementary material Fig. S4A). These foci are often accompanied by bright foci upon DAPI staining (supplementary material Fig. S4A, panels 2 and 3). Since it was shown that Ki-67 interacts with the heterochromatin protein HP1 (Kametaka et al., 2002; Scholzen et al., 2002), some pore-free islands would layer over the heterochromatic regions. Consistent with this observation, we also found that PCNA foci in the mid-to-late S phase, which are associated with the late-replicated heterochromatic regions (Dimitrova et al., 1999; O'Keefe et al., 1992), are often located in the small pore-free areas (supplementary material Fig. S4B). Such peripheral heterochromatin layers and the highly accumulated filamentous meshwork of lamin A/C might inhibit novel pore formation, creating the pore-free islands. Alternatively, this kind of stable and rigid structure might also prevent the migration of neighboring nuclear pores into the pore-free islands.

It is notable that the relationship between lamin A/C and nuclear pores is maintained throughout the cell cycle (supplementary material Fig. S1B). Accordingly, the dynamic change(s) in pore distribution described here could be triggered by a cell-cycle-specific reorganization of lamin A/C, which might be coupled with rearrangements in the heterochromatin layer beneath. In fact, it was reported that large-scale chromosomal movements indeed occur within the nuclei during the progression of G1 phase (Csink and Henikoff, 1998; Walter et al., 2003).

Of particular interest is the difference in pore distribution between the quiescence (G0) and replicative senescence of human fibroblast IMR90 (Fig. 7A): whereas, in the quiescent cells, they remain patched pattern similar to those of G1 nuclei, the senescent cells have a much more uniform distribution, with a higher density of pores (Fig. 7A). Since both are in a 'non-dividing' state, such striking difference might reflect their distinct physiological activity or metabolism.

Physiological relevance of the pore-free islands

Why do pore-free islands exist? First, an apparent effect of the pore-free islands on the nuclear envelope is to create nuclear regions that will be deficient in nucleocytoplasmic transport. This might have drastic effects on many aspects of local nuclear functions if there are any transcription-coupled mRNA export systems, such as those proposed in yeast (Rodriguez-Navarro et al., 2004; Vinciguerra and Stutz, 2004). Indeed, inside the HeLa S3 cells, nuclei are closely surrounded with ER and Golgi apparatus spreading into the edge of the cells. The pore-free islands are, however, excluded from such organelles (supplementary material Fig. S5A), suggesting an optimal cellular architecture of HeLa S3 cells for an efficient transport system. Second, recent publications demonstrate some direct connections between nuclear pores and gene regulation, via nucleoporin and gene-promoter interactions upon transcriptional activation (Casolari et al., 2004; Ishii et al., 2002; Schmid et al., 2006). In fact, the pore-free islands comprise vast heterochromatin regions, which are normally gene silent, beneath them (supplementary material Fig. S4). Pore-rich and pore-poor subdomains on the nuclear envelope might reflect gene(s) activation and silencing states of the corresponding nuclear surface of certain chromosome territories. Indeed, levels of in vivo incorporation of BrUTP in nuclei with large pore-free islands was significantly lower than the nuclei with uniform pore distribution, suggesting a correlation between nuclear pore density and transcriptional activity (supplementary material Fig. S5B).

With the newly identified subdomain (island) of the nuclear envelope, we could also follow the dynamics of nuclei. In HeLa cells, the pore-free islands localize on both sides of the telophase nuclei (Fig. 3A). In G1 nuclei, the pore-free islands are confined on their top and bottom (Fig. 3A). This drastic change of the pore-free island positioning is considered to be a consequence of a dynamic movement of the nuclei during the early cell-cycle stages.

In conclusion, nuclear envelope subdomains, represented by lamin-A/C-enriched pore-free islands, were identified in all the human cell lines examined. Their regulation in cell cycle-dependent dynamics would be controlled by the reorganization of inner nuclear structures. Such general periodic dynamics of subdomain might reflect yet undefined nuclear functions.

Materials and Methods

Cells and antibodies

HeLaS3, HeLa, IMR90 were purchased from Dainippon Seiyaku (Japan), RIKEN Cell Bank (Japan), Japan Health Sciences Foundation. HeLaS3, HeLa, IMR90 and U-2 OS cells were all grown in DMEM medium (Sigma) containing 10% fetal bovine serum (Gibco-BRL) at 37°C in 5% CO_2. For IMR90 human normal diploid fibroblast, non-essential amino acids (Sigma) were added to the culture medium. For cell synchronization, HeLaS3 cells were blocked by nocodazol (Sigma) at a concentration of 0.1 μg/ml for 4 hours. Mitotic cells were recovered by shaking off, washed three times with PBS and seeded again onto poly-L-lysine-coated coverslips. The cell-cycle profile of the synchronized cells was examined by Olympus LCS2 (Olympus, Japan).

Anti-lamin A/C (SC7292), anti-lamin B (SC6216) and anti-PCNA (SC7907) antibodies were purchased from Santa Cruz Biotechnology. Anti-emerin rabbit serum was kindly provided by K. Wilson (Johns-Hopkins University, Baltimore, MD). mAb414 (ab24609) and anti-human CENP-F (ab5) antibody were obtained from Abcom. Anti-lap2β (611000), LBR (1398-1) and Ki-67 (NA59) antibodies were from BD Transduction Laboratories, Epitomics and Oncogene, respectively. Preparation of monoclonal antibody against p62, MAb 2A11, is described below. Both monoclonal antibodies, MAb 2A11 and MAb414, gave the same staining patterns of nuclear pores in all figures presented in this study.

The anti-p62 rat monoclonal antibody was generated as follows, mainly based on the rat lymph node method established by Kishiro et al. (Kishiro et al., 1995). A ten-week-old female WKY/NCrj rat (Charles River) was immunized with an emulsion containing recombinant GST-fused human p62 (1-300 aa) protein and Freund's complete adjuvant. After 3 weeks, the cells from the lymph nodes of a rat immunized with an antigen were fused with mouse myeloma Sp2/0-Ag14 cells. At 10 days post fusion, the hybridoma supernatants were screened by means of ELISA against recombinant GST-fused human p62 protein. Positive clones were subcloned and rescreened by immunoblotting and immunostaining. Finally, a monoclonal antibody, clone 2A11, was selected. The mAb 2A11 was found to be an IgG1(κ) subtype via the use of a rat antibody isotyping kit.

Immunofluorescence staining of cells

HeLaS3, HeLa, IMR90 and U-2 OS cells were grown on coverslips coated with poly-L-lysine (Wako, Japan). Immunofluorescence was carried out as described (Maeshima et al., 2005; Maeshima and Laemmli, 2003) with minor modifications. All the operations were performed at room temperature. The cells were washed in PBS and fixed with freshly prepared 2% paraformaldehyde in PBS for 15 minutes. The fixed cells were then treated with 50 mM glycine in HMK buffer (20 mM HEPES, pH 7.5, 1 mM $MgCl_2$, 100 mM KCl) for 5 minutes, rinsed with HMK (5 minutes), and permeabilized with 0.5% Triton X-100 (Calbiochem) in HMK for 5 minutes. After washing for 5 minutes with HMK, the cells were incubated with 10% normal goat serum (NGS) (Chemicom) in HMK for 30 minutes. The cells were incubated with the first antibody in HMK buffer containing 1% NGS for 1 hour. The antibody dilution rates used in this experiment were as follows: 1:400 for anti-p62, 1:5000 for Mab414, 1:2000 for emerin and laminA/C, 1:1000 dilution for lap2β, PCNA, Ki67 and CENP-F. After washing with HMK (five times for 3 minutes), the cells were incubated with 1:500-1:1000 goat Alexa Fluor 488 and/or 594 antibody (Invitrogen) in HMK buffer containing 1% NGS for 1 hour. After extensive washing with HMK (five times for 3 minutes), followed by counterstaining with 1 μg/ml DAPI (Roche), coverslips were mounted in PPDI [20 mM HEPES, pH 7.4, 1 mM $MgCl_2$, 100 mM KCl, 78% glycerol, 1 mg/ml paraphenylene diamine (Sigma)] and sealed with nail polish.

In some experiments, to visualize PCNA foci associated with DNA replication, before fixation, HeLa cells were extracted with 0.5% Triton X-100 in ice-cold CSK buffer [10 mM HEPES-KOH, pH 7.5, 300 mM sucrose, 100 mM NaCl, 3 mM $MgCl_2$, 100 nM Microcystin LR (Calbiochem) and 0.1 mM PMSF (Sigma)] for 2 minutes and washed with the same ice-cold buffer without Triton X-100 (twice for 3 minutes). Subsequent operations were carried out as described above. For the anti-lamin B antibody that did not work for the immunostaining of paraformaldehyde-fixed samples, a protocol that allows the retrieval of masked or hidden epitopes was used after fixation and permeabilization (Peranen et al., 1993).

Image stacks were recorded with a DeltaVision microscope (Applied Precision) using a step size of 0.2 μm. The objective used was an Olympus 100×/1.35 UPlanApo (Olympus). In the image stacks obtained as described above, optical sections including the nuclear surfaces that are close to the coverslips, are shown in the figures because this makes it possible to display a number of nuclear surfaces on the same focal plain. It should be noted that all the images are shown without deconvolution. The chromatic aberration in the *Z*-axis was corrected by shifting the different channels relative to each other as described by Maeshima and Laemmli (Maeshima and Laemmli, 2003). The measured chromatic shift was 0.4 μm between the blue and green channel and 0.6 μm between the blue and red channel. These values were obtained with the help of three-color beads of 0.1 μm diameter (Molecular Probes). The lateral chromatic aberration was measured to be negligible. To determine density of nuclear pores, the number of nuclear pores in two different areas of 25 μm^2 on each nuclear surface in five independent cells was counted and used to get average density of nuclear pores. The average density of nuclear pores is shown with standard deviation.

Scanning electron microscopy

Synchronized mitotic cells (see above) were seeded onto poly-L-lysine-coated metal specimen holders and cultured for 3 hours. The cells on the specimen holders were frozen rapidly in liquid propane (–184°C), fractured in a cryo-transfer system at –120°C (Alto-2500, Oxford, Oxon, UK). The fractured cells were coated by Cr and observed by FE-SEM (LE01530, LEO, Oberkochen, Germany).

Knockdown of laminA/C and emerin by siRNA in HeLa S3 cells

Pre-annealed dsRNAs were purchased from Qiagen. The siRNA sequences targeting lamin A/C and emerin are as follows: lamin A/C (CUGGACUUCCAGAAGAACA-dTT based on accession number NM_005572) and emerin (CCGUGCUCC-UGGGGCUGG GdTT, based on NM_000117). siRNA transfection was carried out essentially described as Harborth et al. (Harborth et al., 2001) with minor modifications as follows: The day before transfection, 0.3×10^5 HeLa S3 cells were seeded onto poly-L-lysine-coated coverslips in 12-well plates (2 ml per well). The transient transfection of siRNAs was carried out using Oligofectamine (GibcoBRL). 48 μl Opti-MEM1 medium (GibcoBRL) and 12 μl Oligofectamine per well were preincubated for 5-10 minutes at room temperature and 200 μl Opti-MEM 1 medium were mixed with 12 μl siRNA. The two mixtures were combined and incubated for 20 minutes at room temperature for complex formation. The entire mixture was added to the seeded cells with a final concentration of 100 nM for the siRNAs. Cells were typically assayed 48-72 hours after transfection by immunofluorescence. In some cases, to prevent the transfected cells from becoming confluent, the cells were diluted fourfold and seeded again onto coverslips 24 hours after transfection. The cell cycle profile of the lamin A/C knockdown cells was examined by Olympus LCS2 (Olympus, Japan) and shown as histograms of DNA content.

Construction of plasmid

Lamin A cDNA was amplified from a cDNA library by PCR. The cDNA library was synthesized from HeLaS3 total RNAs by Super-Script III (Invitrogen). The PCR primers used are as follows: 5′-CTGGCAACCTGCCGGCCATG-3′ and 5′-GTCCCAGATTACATGATGCT-3′. Amplified fragments were cloned and sequenced for verification.

An expression clone, pEXPR-EF-1α–Venus-laminA, was constructed using the multi-site Gateway system, essentially as described previously (Sasaki et al., 2004; Yahata et al., 2005). In brief, a destination vector, pEF5/FRT/V5-DEST (Invitrogen), carrying the EF-1α promoter, was used with two entry clones, pENTR-L1-SDK-Venus (no stop)-GGSGGT-L3 and pENTR-R3r-LaminA (stop)-L2, to obtain clone encoding chimera of Venus fused at the N-terminal site of LaminA. Two entry clones, pENTR-L1-SDK-Venus (no stop)-GGSGGT-L3 and pENTR-R3r-LaminA (stop)-L2, were constructed from Venus and Lamin A cDNAs amplified from pCS2-Venus and lamin A clone (Nagai et al., 2002) (above) and donor vectors, pDONR-P1P3r (for Venus) and pDONR-P3P2 (for Lamin A), using BP reactions. Sequences of entry clones were verified using ABI PRISM® 3100 Genetic Analyzer (Applied Biosystems).

Transient expression of Venus-lamin A and Venus-p62 in HeLa cells

For transfection of the plasmid, Effectene (Qiagen) was used according to the instruction manual. For ectopic expression experiments of lamin A (Fig. 6), at 48 hours after transfection, the pore distribution on the nuclear surface was examined by the nuclear pore staining as described above.

Mathematical consideration of the pore-free islands

If the pore distributions on the nuclear surface are assumed to occur at random, and to follow a Poisson Distribution, the probability of number of nuclear pores (k) on area S (μm^2) is $P(k; \lambda S)=\exp[-\lambda S](\lambda S)^k/k!$, where λ is the expected number of occurrences, that is, the average pore density. The probability of no nuclear pores in area S is $P(0; \lambda S)=\exp[-\lambda S]$. Since a typical area of pore-free island in the G1 phase is about 30 μm^2 and average pore density in the nucleus is about 7 NPCs/μm^2, the probability of such a pore-free island occurring by chance, is about 1×10^{-79}.

We are grateful to Drs Kas and Goldfarb for critical reading of this manuscript, to Dr Yoshida for access to his DeltaVision and to Ms. Asakawa for her competent technical assistance. We thank Dr Wilson for her generous gift of the antibody and Drs Nagai and Miyawaki for providing Venus cDNAs, Drs Martin-Lluesma and Habu for technical advice on siRNA, Dr Hiraoka for the mathematical consideration of the pore-free islands, Dr Mizuno for PCNA staining, Dr Takagi for advice about Ki-67, and members of Cellular Dynamics Lab for helpful discussion. We also thank Dr Feather for editing the manuscript. K.M. was supported by Special Postdoctoral Program in RIKEN. This work was supported by a MEXT grant-in-aid, RIKEN Special Project Funding for Basic Science (Chemical Biology Research Project and Bioarchitect Project) and RIKEN R&D.

References

Aebi, U., Cohn, J., Buhle, L. and Gerace, L. (1986). The nuclear lamina is a meshwork of intermediate-type filaments. *Nature* **323**, 560-564.

Agrelo, R., Setien, F., Espada, J., Artiga, M. J., Rodriguez, M., Perez-Rosado, A., Sanchez-Aguilera, A., Fraga, M. F., Piris, M. A. and Esteller, M. (2005). Inactivation of the lamin A/C gene by CpG island promoter hypermethylation in

hematologic malignancies, and its association with poor survival in nodal diffuse large B-cell lymphoma. *J. Clin. Oncol.* **23**, 3940-3947.

Broers, J. L. and Ramaekers, F. C. (1994). Differentiation markers for lung-cancer subtypes. A comparative study of their expression in vivo and in vitro. *Int. J. Cancer Suppl.* **8**, 134-137.

Burke, B. and Stewart, C. L. (2002). Life at the edge: the nuclear envelope and human disease. *Nat. Rev. Mol. Cell Biol.* **3**, 575-585.

Casolari, J. M., Brown, C. R., Komili, S., West, J., Hieronymus, H. and Silver, P. A. (2004). Genome-wide localization of the nuclear transport machinery couples transcriptional status and nuclear organization. *Cell* **117**, 427-439.

Cronshaw, J. M., Krutchinsky, A. N., Zhang, W., Chait, B. T. and Matunis, M. J. (2002). Proteomic analysis of the mammalian nuclear pore complex. *J. Cell Biol.* **158**, 915-927.

Csink, A. K. and Henikoff, S. (1998). Large-scale chromosomal movements during interphase progression in Drosophila. *J. Cell Biol.* **143**, 13-22.

Daigle, N., Beaudouin, J., Hartnell, L., Imreh, G., Hallberg, E., Lippincott-Schwartz, J. and Ellenberg, J. (2001). Nuclear pore complexes form immobile networks and have a very low turnover in live mammalian cells. *J. Cell Biol.* **154**, 71-84.

Davis, L. I. (1995). The nuclear pore complex. *Annu. Rev. Biochem.* **64**, 865-896.

Dimitrova, D. S., Todorov, I. T., Melendy, T. and Gilbert, D. M. (1999). Mcm2, but not RPA, is a component of the mammalian early G1-phase prereplication complex. *J. Cell Biol.* **146**, 709-722.

Elbashir, S. M., Harborth, J., Lendeckel, W., Yalcin, A., Weber, K. and Tuschl, T. (2001). Duplexes of 21-nucleotide RNAs mediate RNA interference in cultured mammalian cells. *Nature* **411**, 494-498.

Fahrenkrog, B., Koser, J. and Aebi, U. (2004). The nuclear pore complex: a jack of all trades? *Trends Biochem. Sci.* **29**, 175-182.

Gerace, L. and Burke, B. (1988). Functional organization of the nuclear envelope. *Annu. Rev. Cell Biol.* **4**, 335-374.

Goldman, R. D., Gruenbaum, Y., Moir, R. D., Shumaker, D. K. and Spann, T. P. (2002). Nuclear lamins: building blocks of nuclear architecture. *Genes Dev.* **16**, 533-547.

Gorlich, D. and Kutay, U. (1999). Transport between the cell nucleus and the cytoplasm. *Annu. Rev. Cell Dev. Biol.* **15**, 607-660.

Haraguchi, T., Koujin, T., Hayakawa, T., Kaneda, T., Tsutsumi, C., Imamoto, N., Akazawa, C., Sukegawa, J., Yoneda, Y. and Hiraoka, Y. (2000). Live fluorescence imaging reveals early recruitment of emerin, LBR, RanBP2, and Nup153 to reforming functional nuclear envelopes. *J. Cell Sci.* **113**, 779-794.

Haraguchi, T., Koujin, T., Segura-Totten, M., Lee, K. K., Matsuoka, Y., Yoneda, Y., Wilson, K. L. and Hiraoka, Y. (2001). BAF is required for emerin assembly into the reforming nuclear envelope. *J. Cell Sci.* **114**, 4575-4585.

Harborth, J., Elbashir, S. M., Bechert, K., Tuschl, T. and Weber, K. (2001). Identification of essential genes in cultured mammalian cells using small interfering RNAs. *J. Cell Sci.* **114**, 4557-4565.

Hawryluk-Gara, L. A., Shibuya, E. K. and Wozniak, R. W. (2005). Vertebrate Nup53 interacts with the nuclear lamina and is required for the assembly of a Nup93-containing complex. *Mol. Biol. Cell* **16**, 2382-2394.

Hetzer, M. W., Walther, T. C. and Mattaj, I. W. (2005). Pushing the envelope: structure, function, and dynamics of the nuclear periphery. *Annu. Rev. Cell Dev. Biol.* **21**, 347-380.

Hutchison, C. J. and Worman, H. J. (2004). A-type lamins: guardians of the soma? *Nat. Cell Biol.* **6**, 1062-1067.

Hutchison, C. J., Alvarez-Reyes, M. and Vaughan, O. A. (2001). Lamins in disease: why do ubiquitously expressed nuclear envelope proteins give rise to tissue-specific disease phenotypes? *J. Cell Sci.* **114**, 9-19.

Imamoto, N. (2000). Diversity in nucleocytoplasmic transport pathways. *Cell Struct. Funct.* **25**, 207-216.

Ishii, K., Arib, G., Lin, C., Van Houwe, G. and Laemmli, U. K. (2002). Chromatin boundaries in budding yeast: the nuclear pore connection. *Cell* **109**, 551-562.

Kametaka, A., Takagi, M., Hayakawa, T., Haraguchi, T., Hiraoka, Y. and Yoneda, Y. (2002). Interaction of the chromatin compaction-inducing domain (LR domain) of Ki-67 antigen with HP1 proteins. *Genes Cells* **7**, 1231-1242.

Kill, I. R. (1996). Localisation of the Ki-67 antigen within the nucleolus. Evidence for a fibrillarin-deficient region of the dense fibrillar component. *J. Cell Sci.* **109**, 1253-1263.

Kishiro, Y., Kagawa, M., Naito, I. and Sado, Y. (1995). A novel method of preparing rat-monoclonal antibody-producing hybridomas by using rat medial iliac lymph node cells. *Cell Struct. Funct.* **20**, 151-156.

Kubitscheck, U., Wedekind, P., Zeidler, O., Grote, M. and Peters, R. (1996). Single nuclear pores visualized by confocal microscopy and image processing. *Biophys. J.* **70**, 2067-2077.

Lenz-Bohme, B., Wismar, J., Fuchs, S., Reifegerste, R., Buchner, E., Betz, H. and Schmitt, B. (1997). Insertional mutation of the Drosophila nuclear lamin Dm0 gene results in defective nuclear envelopes, clustering of nuclear pore complexes, and accumulation of annulate lamellae. *J. Cell Biol.* **137**, 1001-1016.

Liao, H., Winkfein, R. J., Mack, G., Rattner, J. B. and Yen, T. J. (1995). CENP-F is a protein of the nuclear matrix that assembles onto kinetochores at late G2 and is rapidly degraded after mitosis. *J. Cell Biol.* **130**, 507-518.

Liu, J., Rolef Ben-Shahar, T., Riemer, D., Treinin, M., Spann, P., Weber, K., Fire, A. and Gruenbaum, Y. (2000). Essential roles for Caenorhabditis elegans lamin gene in nuclear organization, cell cycle progression, and spatial organization of nuclear pore complexes. *Mol. Biol. Cell* **11**, 3937-3947.

Macara, I. G. (2001). Transport into and out of the nucleus. *Microbiol. Mol. Biol. Rev.* **65**, 570-594.

Machiels, B. M., Ramaekers, F. C., Kuijpers, H. J., Groenewoud, J. S., Oosterhuis, J. W. and Looijenga, L. H. (1997). Nuclear lamin expression in normal testis and testicular germ cell tumours of adolescents and adults. *J. Pathol.* **182**, 197-204.

Maeshima, K. and Laemmli, U. K. (2003). A two-step scaffolding model for mitotic chromosome assembly. *Dev. Cell* **4**, 467-480.

Maeshima, K., Eltsov, M. and Laemmli, U. K. (2005). Chromosome structure: improved immunolabeling for electron microscopy. *Chromosoma* **114**, 365-375.

Maul, G. G., Price, J. W. and Lieberman, M. W. (1971). Formation and distribution of nuclear pore complexes in interphase. *J. Cell Biol.* **51**, 405-418.

Maul, G. G., Deaven, L. L., Freed, J. J., Campbell, G. L. and Becak, W. (1980). Investigation of the determinants of nuclear pore number. *Cytogenet. Cell Genet.* **26**, 175-190.

Mounkes, L., Kozlov, S., Burke, B. and Stewart, C. L. (2003). The laminopathies: nuclear structure meets disease. *Curr. Opin. Genet. Dev.* **13**, 223-230.

Nagai, T., Ibata, K., Park, E. S., Kubota, M., Mikoshiba, K. and Miyawaki, A. (2002). A variant of yellow fluorescent protein with fast and efficient maturation for cell-biological applications. *Nat. Biotechnol.* **20**, 87-90.

O'Keefe, R. T., Henderson, S. C. and Spector, D. L. (1992). Dynamic organization of DNA replication in mammalian cell nuclei: spatially and temporally defined replication of chromosome-specific alpha-satellite DNA sequences. *J. Cell Biol.* **116**, 1095-1110.

Oberleithner, H., Brinckmann, E., Schwab, A. and Krohne, G. (1994). Imaging nuclear pores of aldosterone-sensitive kidney cells by atomic force microscopy. *Proc. Natl. Acad. Sci. USA* **91**, 9784-9788.

Peranen, J., Rikkonen, M. and Kaariainen, L. (1993). A method for exposing hidden antigenic sites in paraformaldehyde-fixed cultured cells, applied to initially unreactive antibodies. *J. Histochem. Cytochem.* **41**, 447-454.

Rabut, G., Doye, V. and Ellenberg, J. (2004). Mapping the dynamic organization of the nuclear pore complex inside single living cells. *Nat. Cell Biol.* **6**, 1114-1121.

Rodriguez-Navarro, S., Fischer, T., Luo, M. J., Antunez, O., Brettschneider, S., Lechner, J., Perez-Ortin, J. E., Reed, R. and Hurt, E. (2004). Sus1, a functional component of the SAGA histone acetylase complex and the nuclear pore-associated mRNA export machinery. *Cell* **116**, 75-86.

Rout, M. P. and Wente, S. R. (1994). Pores for thought: nuclear pore complex proteins. *Trends Cell Biol.* **4**, 357-365.

Rout, M. P., Aitchison, J. D., Suprapto, A., Hjertaas, K., Zhao, Y. and Chait, B. T. (2000). The yeast nuclear pore complex: composition, architecture, and transport mechanism. *J. Cell Biol.* **148**, 635-651.

Sasaki, Y., Sone, T., Yoshida, S., Yahata, K., Hotta, J., Chesnut, J. D., Honda, T. and Imamoto, F. (2004). Evidence for high specificity and efficiency of multiple recombination signals in mixed DNA cloning by the Multisite Gateway system. *J. Biotechnol.* **107**, 233-243.

Schmid, M., Arib, G., Laemmli, C., Nishikawa, J., Durussel, T. and Laemmli, U. K. (2006). Nup-PI: the nucleopore-promoter interaction of genes in yeast. *Mol. Cell* **21**, 379-391.

Scholzen, T., Endl, E., Wohlenberg, C., van der Sar, S., Cowell, I. G., Gerdes, J. and Singh, P. B. (2002). The Ki-67 protein interacts with members of the heterochromatin protein 1 (HP1) family: a potential role in the regulation of higher-order chromatin structure. *J. Pathol.* **196**, 135-144.

Smythe, C., Jenkins, H. E. and Hutchison, C. J. (2000). Incorporation of the nuclear pore basket protein nup153 into nuclear pore structures is dependent upon lamina assembly: evidence from cell-free extracts of Xenopus eggs. *EMBO J.* **19**, 3918-3931.

Stadelmann, B., Khandjian, E., Hirt, A., Luthy, A., Weil, R. and Wagner, H. P. (1990). Repression of nuclear lamin A and C gene expression in human acute lymphoblastic leukemia and non-Hodgkin's lymphoma cells. *Leuk. Res.* **14**, 815-821.

Stuurman, N., Heins, S. and Aebi, U. (1998). Nuclear lamins: their structure, assembly, and interactions. *J. Struct. Biol.* **122**, 42-66.

Sullivan, T., Escalante-Alcalde, D., Bhatt, H., Anver, M., Bhat, N., Nagashima, K., Stewart, C. L. and Burke, B. (1999). Loss of A-type lamin expression compromises nuclear envelope integrity leading to muscular dystrophy. *J. Cell Biol.* **147**, 913-920.

Suntharalingam, M. and Wente, S. R. (2003). Peering through the pore: nuclear pore complex structure, assembly, and function. *Dev. Cell* **4**, 775-789.

Vasu, S. K. and Forbes, D. J. (2001). Nuclear pores and nuclear assembly. *Curr. Opin. Cell Biol.* **13**, 363-375.

Venables, R. S., McLean, S., Luny, D., Moteleb, E., Morley, S., Quinlan, R. A., Lane, E. B. and Hutchison, C. J. (2001). Expression of individual lamins in basal cell carcinomas of the skin. **84**, 512-519.

Vinciguerra, P. and Stutz, F. (2004). mRNA export: an assembly line from genes to nuclear pores. *Curr. Opin. Cell Biol.* **16**, 285-292.

Walter, J., Schermelleh, L., Cremer, M., Tashiro, S. and Cremer, T. (2003). Chromosome order in HeLa cells changes during mitosis and early G1, but is stably maintained during subsequent interphase stages. *J. Cell Biol.* **160**, 685-697.

Wilson, K. L. (2000). The nuclear envelope, muscular dystrophy and gene expression. *Trends Cell Biol.* **10**, 125-129.

Yahata, K., Kishine, H., Sone, T., Sasaki, Y., Hotta, J., Chesnut, J. D., Okabe, M. and Imamoto, F. (2005). Multi-gene gateway clone design for expression of multiple heterologous genes in living cells: conditional gene expression at near physiological levels. *J. Biotechnol.* **118**, 123-134.